Published in final edited form as:

J Biomech Eng. 2015 August ; 137(8): 084501. doi:10.1115/1.4030311.

Analysis of the Constraint Joint Loading in the Thumb During Pipetting

John Z. Wu,
National Institute for Occupational Safety and Health, 1095 Willowdale Road, MS-2027, Morgantown, WV 26505

Erik W. Sinsel,
National Institute for Occupational Safety and Health, 1095 Willowdale Road, MS-2027, Morgantown, WV 26505

Kristin D. Zhao,
Biomechanics Laboratory, Division of Orthopedic Research, Mayo Clinic, Rochester, MN 55905

Kai-Nan An, and
Biomechanics Laboratory, Division of Orthopedic Research, Mayo Clinic, Rochester, MN 55905

Frank L. Buczek
Lake Erie College of Osteopathic Medicine (LECOM), Erie, PA 16509

John Z. Wu: jwu@cdc.gov

Abstract

Dynamic loading on articular joints is essential for the evaluation of the risk of the articulation degeneration associated with occupational activities. In the current study, we analyzed the dynamic constraint loading for the thumb during pipetting. The constraint loading is considered as the loading that has to be carried by the connective tissues of the joints (i.e., the cartilage layer and the ligaments) to maintain the kinematic constraints of the system. The joint loadings are solved using a classic free-body approach, using the external loading and muscle forces, which were obtained in an inverse dynamic approach combined with an optimization procedure in ANYBODY. The constraint forces in the thumb joint obtained in the current study are compared with those obtained in the pinch and grasp tests in a previous study (Cooney and Chao, 1977, "Biomechanical Analysis of Static Forces in the Thumb During Hand Function," J. Bone Joint Surg. Am., **59**(1), pp. 27–36). The maximal compression force during pipetting is approximately 83% and 60% greater than those obtained in the tip pinch and key pinch, respectively, while substantially smaller than that obtained during grasping. The maximal lateral shear force is approximately six times, 32 times, and 90% greater than those obtained in the tip pinch, key pinch, and grasp, respectively. The maximal dorsal shear force during pipetting is approximately 3.2 and 1.4 times greater than those obtained in the tip pinch and key pinch, respectively, while substantially smaller than that

Correspondence to: John Z. Wu, jwu@cdc.gov.

obtained during grasping. Our analysis indicated that the thumb joints are subjected to repetitive, intensive loading during pipetting, compared to other daily activities.

Keywords

ergonomics; thumb; joint force; joint moment; pipette; modeling

1 Introduction

Osteoarthritis (OA) is a common joint disease that frequently involves joints of the hand. A survey study indicated that the presence of radiographic OA in at least one hand joint reaches 67% in women and 55% in men among individuals older than 55 years [1]. In a separate study [2,3], the prevalence of radiographic hand OA in older populations was found to be as high as 85% in women and 75% in men. The thumb carpometacarpal (CMC) joint is the second most frequent hand joint for OA, second to the distal interphalangeal (DIP) joint of the index finger [1,4]. The top joint-specific hand OA prevalence rates are in the second DIP, first CMC, and third proximal interphalangeal (PIP) and reach about 35%, 21%, and 18%, respectively [4]. Although hand OA has been linked to numerous factors, mechanical loading was identified as one of the most important risk factors [5]. Moderate hand use is found to be beneficial to the finger joints [6], whereas extensive, repeated loading will induce joint degeneration [7]. Strong evidence has linked the initiation and development of OA in the CMC joint to occupational activities that require repeated, forceful thumb motions [8]. Despite numerous epidemiological studies, joint loading of the thumb associated with the occupational activities has not been quantified.

There are limited studies to quantify joint loading in the thumb in the literature. Cooney and Chao [9] analyzed the thumb joint loading during static pinch and grasp using five cadaver specimens. They found that the joint contact force in interphalangeal (IP), metacarpophalangeal (MP), and CMC joint reached 29.4 N, 52.9 N, and 117.6 N, respectively, in simple pinch with an applied force of 9.8 N. The compressive force in the CMC joint reached as great as 1176 N during strong grasp tests. Their analysis indicated that the CMC joint is subjected to substantial loading in normal activities and this coincides with the high OA prevalence rate in epidemiological studies.

One occupational activity that exposes workers to repetitive, forceful loading of the thumb is the use of thumb-push manual pipettes, which are widely used in laboratories of medical, biological, and chemical research. The force applied to the pipette or musculoskeletal loading while pipetting has been rarely quantified in previous studies. Fredriksson [10] investigated the relationship between the push forces at the thumb required to operate a pipette and the participants' thumb strength. Asundi et al. [11] performed more extensive biomechanical analysis; they measured the thumb push force and electromyography (EMG) activities in four extrinsic muscles for different pipetting tasks. The dynamic forces applied on the thumb joints during pipetting have not been evaluated.

Our previous study [12] indicated that the compression force at the plunger button during pipetting reaches the magnitudes observed in other activities, such as pinching [13] and jar

opening [14]. Considering the repetitive loading nature during pipetting, the thumb joints may experience excessive loading compared to those in other occupational or daily activities. In order to assess the risk of articulation degeneration associated with the pipette operation, it is necessary to evaluate the dynamic loading on the articular joint. The goal of the current study was to characterize the dynamic loading in the thumb joints during pipetting. Our hypothesis is that maximal joint loading during pipetting will occur in the CMC joint of the thumb.

2 Methods

2.1 Test Setup and Experimental Design

The test-setup is similar to that used in our previous study [12]. A typical thumb-activated pipette (P200, Pipetman, Gilson, Inc, Middleton, WI) was instrumented and utilized in the tests (Fig. 1(*a*)). A miniature force sensor (Series LBS-111 N, Interface Inc., Scottsdale, AZ) was installed under the plunger button to measure the plunger force. Kinematics for the thumb, fingers, hand, and forearm were determined using methods similar to those in previous studies [12,15,16]. Briefly, three semispherical, retroreflective markers (4 mm diameter) were placed on each of the finger/thumb/hand segments using a thin self-adhesive tape (Fig. 1(*a*)). Motion capture markers were placed on the plunger press button and the pipette handle to determine relative displacement of the plunger button. Twelve finger segments, three thumb segments, a hand, and a forearm segment were considered in the kinematic analysis. The motion marker trajectories were recorded by using a 14-camera Vicon Nexus system (Oxford Metrics Ltd., Oxford, UK) at 100 Hz. Kinematic data were collected from eight subjects. All eight subjects were right-handed, experienced laboratory technicians. During the tests, the subjects were instructed to extract the fluid from one container on their left side and dispense it to another container on their right side. In the extraction action, the subjects pressed the plunger button to the first stop and extracted the fluid by releasing the button; in the dispensing action, the subjects depressed the plunger button to the second stop to completely dispense the fluid. No particular pipetting rate was set for the subjects. The study protocol was approved by the NIOSH HSRB (Human Subjects Review Board, National Institute for Occupational Safety and Health).

2.2 Multibody Dynamical Modeling of Pipetting

The hand model is similar to that used in our previous studies [12,17]. Briefly, the hand is modeled as a multibody linkage system and includes four fingers (index, long, ring, and little finger), a thumb, a palm, and a forearm segment (Fig. 1(*b*)). Each of the fingers is comprised of a distal, intermediate, and proximal phalanx, and a metacarpal, which are linked by three joints (i.e., DIP, PIP, and metacarpophalangeal (MCP) joints). The thumb is comprised of a distal and proximal phalanx, a metacarpal bone, and a trapezium, which are also linked by three joints (i.e., IP, MP, and CMC joints). The current study is focused on the thumb; therefore, it includes only nine muscles that are attached to the thumb (i.e., flexor pollicis longus, extensor pollicis longus, extensor pollicis brevis, abductor pollicis longus, flexor pollicis brevis, abductor pollicis brevis, the transverse head of the adductor pollicis, the oblique head of the adductor pollicis, and opponens pollicis (OPP)). The hand model was developed on the platform of the commercial software package ANYBODY (version 5.0;

AnyBody Technology, Aalborg, Denmark). The dimensions of the thumb and finger segments of each subject have been measured and applied to scale the model. However, generic muscle/tendon models and parameters were applied for all subjects. The muscle forces were calculated using an inverse dynamic approach combined with an optimization procedure in ANYBODY, in which the maximal normalized muscle force is minimized [12,17]. The time-histories of each joint angle and the interface contact force between the thumb tip and the pipette's dispense plunger button were applied as model input, whereas the corresponding time-histories of the excursions and forces of muscle–tendon units of the thumb were predicted.

2.3 Calculation of Joint Loading of the Thumb

After all muscle forces are calculated, the joint loadings are solved using a classic free-body approach, similar to that applied by Cooney and Chao [9]. The muscle forces and joint loadings of each subject were calculated individually. The joint constraint loadings are the forces and moments that the joints have to withstand to enforce the kinematic constraints of the system.

The IP joint has one degree-of-freedom (DOF) (flexion/extension). The joint applies two rotational constraints (adduction/abduction and internal/external rotations) and three translational constraints to the system, consequently, and it has to resist two constraint moments (M_x and M_y) and three constraint forces (R_x, R_y, and R_z). The constraint forces and moments in the IP joint are solved by an equilibrium considering only the distal phalanx, as illustrated in Fig. 2. The forces in the muscles across the IP joint and the external forces applied on the segment are considered in the calculations. The compressive constraint force (R_x) is applied on the cartilage layer, whereas the dorsal (R_y) and radial (R_z) shear forces are carried by the ligaments. The joint constraint moments, M_x and M_y, are to withstand the axial (internal/external rotation) and the lateral (radial) bending, respectively.

The MP joint has two DOFs (flexion/extension and adduction/abduction); and it applies one rotational (internal/external rotation) and three translational constraints to the system; correspondingly, it has one constraint moment (M_x) and three constraint forces (R_x, R_y, and R_z). The constraint forces and moments in the MP are solved by an equilibrium, as illustrated in Fig. 3, in which the distal and middle phalanx are considered. The forces in the muscles across the MP joint and the external forces applied on the segments are considered in the calculations.

The CMC joint has three DOFs (flexion/extension, adduction/abduction, and internal/external rotation). It applies three translational constraints to the system, consequently, it has only three constraint forces (R_x, R_y, and R_z). The constraint forces in the CMC joint are solved by an equilibrium as illustrated in Fig. 4, in which the distal, middle, and proximal phalanx are considered. The forces in the muscles across the CMC joint and the external forces applied on the three segments are considered in the calculations.

3 Results

Since the extraction and dispensing actions are cyclic in nature, the time-histories of the plunger displacement and push force, as well as all calculated parameters, are summarized in terms of task cycle, as traditionally treated in the gait analysis [18,19]. The entire work cycle has been divided into the extraction and dispensing cycles. The mean time period of the extraction and dispensing task was 1.98(standard deviation 0.49) s and 1.96(standard deviation 0.41) s, respectively. All forces and moments are presented in positive values or in magnitude.

The plunger push force and displacement as a function of the task cycle is shown in Figs. 5(*a*) and 5(*b*), respectively. The peak push force for the extraction and dispensing cycles was approximately 7 N and 25 N, respectively, and occurred at 59% and 75% work cycle.

The calculated lateral and dorsal shear force and contact force as a function of the work cycle for the CMC joint are shown in Fig. 6. The joint constraint force is predominantly in the axial direction. The mean lateral and dorsal shear force, and mean contact force reached approximately 33 N, 133 N, and 166 N, respectively; all occurred around 75% of the dispensing cycle.

The calculated lateral and dorsal shear force and contact force as a function of the work cycle for the MP joint are shown in Fig. 7. The joint constraint force in the MP joint is similar in both trend and magnitude to those in the CMC joint. The mean lateral and dorsal shear force, and mean contact force reached approximately 47 N, 128 N, and 178 N, respectively; all occurred around 75% of the dispensing cycle.

The calculated lateral and dorsal shear force and contact force as a function of the work cycle for the IP joint are shown in Fig. 8. The joint constraint force in the IP joint is substantially smaller than those observed in the MP and CMC joints. The mean lateral and dorsal shear force, and mean contact force reached approximately 34 N, 30 N, and 59 N, respectively; all occurred around 75% of the dispensing cycle.

The magnitude of the joint constraint forces as a function of the work cycle for the CMC, MP, and IP joints are shown in Fig. 9. The peak value of the constraint force occurred near 75% of dispensing cycle and reached approximately 222 N, 225 N, and 74 N in CMC, MP, and IP joints, respectively.

The axial constraint moment in MP joint, the lateral bending and axial constraint moment in IP joint are plotted as a function of the work cycle in Fig. 10. The maximal constraint moment was found to be 0.62 N m in the MP axial constraint. The peak bending and axial constraint moment in IP was 0.23 N m and 0.16 N m, substantially smaller that that in the MP joint.

4 Discussion and Conclusion

The function of the thumb for daily activities requires that it generates enough power and, at the same time, maintains mechanical stability. Strength is generated by the coordinated

action of the muscle/tendon forces, while the stability is maintained by the constraining forces of the joint capsule and ligaments and the contact forces across the articular cartilage. Excessive and repeated loading at the thumb during pipetting will potentially cause excessive constraining forces and contact forces in the MP and CMC joints—factors generally accepted to be associated with the initiation of joint degeneration and OA. Thus, the current model and the analysis would provide a biomechanical foundation for the ergonomic tool design to reduce occupational injuries.

The constraint forces in the thumb joint obtained in the current study are compared with those obtained in the pinch and grasp tests by Cooney and Chao [9] (Table 1). The maximal constraint forces during pipetting were found in different DOFs than those observed in pinch and grasp tests.

The maximal compression force during pipetting obtained in the current study is 178 N, which is approximately 83% and 60% greater than those obtained in the tip pinch (97.3 N) and key pinch (111.4 N), respectively, while substantially smaller than that obtained in grasp (1223 N) [9] (Table 1, right column). The trend of our results differs from the previous study in that the maximal compressive force was found in the MP joint (178 N) and was close in magnitude to that in the CMC joint (160 N), whereas the maximal compressive force was predominantly in the CMC joint in the previous study. The ratio of the maximal joint force to the force applied at the thumb tip for the current study was approximately 9, which is smaller than that observed in the tip pinch (16), key pinch (19.5), and grasp tests (14.4) [9]. Due to the repetitive loading nature during pipetting, the cartilage layer in the CMC and MP joints may be subjected to substantially higher compressive loading intensity than in other daily activities, such as pinch and grasp. Ateshian et al. [20] showed that the forces produced by lateral pinch are generally concentrated at the same region where cartilage thinning is most often observed in cadavers, indicating that the compressive stress in cartilage of the CMC joint could be a significant precursor to articular joint degeneration. Therefore, prolonged pipetting operation could increase the risk of the CMC joint degenerations.

The maximal lateral shear force during pipetting in the current study is found to be 133 N, observed in the CMC joint, which is approximately six times, 32 times, and 90% greater than those obtained in the tip pinch (19 N), key pinch (4 N), and grasp (69 N) [9], respectively. The maximal dorsal shear force during pipetting is found to be 47 N in the MP joint, which is approximately 320% and 140% greater than those obtained in the tip pinch (11 N) and key pinch (19 N), respectively, while substantially smaller than that obtained in grasp (200 N) [9].

The lateral and dorsal shear forces are carried by the ulnar collateral ligaments (UCL), radial collateral ligament (RCL), and the joint capsules. UCL and RCL injuries are common in occupational and sports activities [21–23]. Although the magnitude of the lateral shear forces observed in our study is far less than the level that would cause the ligament to rupture [24], the repetitive loading may potentially induce degenerative adaptation of the UCL and RCL. The anterior oblique ligament, UCL, and RCL have been described as primary dynamic stabilizers of the thumb, especially during pinch and opposition of the

thumb [25]. Intensive, repetitive loading on these ligaments may cause inflammation and laxity of the ligaments, leading to the CMC joint instability, which is considered as a precursor to the degeneration of the joint [26,27].

The constraint loading is considered as the loading that has to be carried by the connective tissues of the joints (i.e., the cartilage layer and the ligaments) to maintain the kinematic constraints of the system. Excessive constraint loading of the joints may induce degeneration of the cartilage layer, laxity of the ligaments, and joint instability, leading to the development of OA at the thumb. Our analysis indicated that the thumb joints are subjected to repetitive, intensive loading during pipetting, compared to other daily activities.

Acknowledgment

We want to express our gratitude to Mr. Dan Welcome (NIOSH) and Dr. Justin F. Shroyer. Mr. Welcome provided technical assistance for the test setup and constructed the digital 3D pipette model; and Dr. Shroyer helped with the subject test and the data processing. Mention of product and/or company name does not imply endorsement by the National Institute for Occupational Safety and Health. The findings and conclusions in this report are those of the authors and do not necessarily represent the views of the National Institute for Occupational Safety and Health.

References

1. Dahaghin S, Bierma-Zeinstra SM, Ginai AZ, Pols HA, Hazes JM, Koes BW. Prevalence and Pattern of Radiographic Hand Osteoarthritis and Association With Pain and Disability (the Rotterdam Study). Ann. Rheum. Dis. 2005; 64(5):682–687. [PubMed: 15374852]
2. Zhang Y, Niu J, Kelly-Hayes M, Chaisson CE, Aliabadi P, Felson DT. Prevalence of Symptomatic Hand Osteoarthritis and Its Impact on Functional Status Among the Elderly: The Framingham Study. Am. J. Epidemiol. 2002; 156(11):1021–1027. [PubMed: 12446258]
3. Zhang Y, Xu L, Nevitt MC, Niu J, Goggins JP, Aliabadi P, Yu W, Lui LY, Felson DT. Lower Prevalence of Hand Osteoarthritis Among Chinese Subjects in Beijing Compared With White Subjects in the United States: The Beijing Osteoarthritis Study. Arthritis Rheum. 2003; 48(4):1034–1040. [PubMed: 12687546]
4. Wilder FV, Barrett JP, Farina EJ. Joint-Specific Prevalence of Osteoarthritis of the Hand. Osteoarthritis Cartilage. 2006; 14(9):953–957. [PubMed: 16759885]
5. Kalichman L, Hernandez-Molina G. Hand Osteoarthritis: An Epidemiological Perspective. Semin. Arthritis Rheum. 2010; 39(6):465–476. [PubMed: 19482338]
6. Solovieva S, Vehmas T, Riihimaki H, Luoma K, Leino-Arjas P. Hand Use and Patterns of Joint Involvement in Osteoarthritis. A Comparison of Female Dentists and Teachers. Rheumatology (Oxford). 2005; 44(4):521–528. [PubMed: 15728421]
7. Hadler NM, Gillings DB, Imbus HR, Levitin PM, Makuc D, Utsinger PD, Yount WJ, Slusser D, Moskovitz N. Hand Structure and Function in an Industrial Setting. Arthritis Rheum. 1978; 21(2): 210–220. [PubMed: 637887]
8. Winzeler S, Rosenstein BD. Occupational Injury and Illness of the Thumb. Causes and Solutions. AAOHN J. 1996; 44(10):487–492. [PubMed: 9043212]
9. Cooney WPR, Chao EY. Biomechanical Analysis of Static Forces in the Thumb During Hand Function. J. Bone Joint Surg. Am. 1977; 59(1):27–36. [PubMed: 833171]
10. Fredriksson K. Laboratory Work With Automatic Pipettes: A Study on How Pipetting Affects the Thumb. Ergonomics. 1995; 38(5):1067–1073. [PubMed: 7737101]
11. Asundi KR, Bach JM, Rempel DM. Thumb Force and Muscle Loads are Influenced by the Design of a Mechanical Pipette and by Pipetting Tasks. Hum. Factors. 2005; 47(1):67–76. [PubMed: 15960087]
12. Wu JZ, Sinsel EW, Gloekler DS, Wimer BM, Zhao KD, An KN, Buczek FL. Inverse Dynamic Analysis of the Biomechanics of the Thumb While Pipetting: A Case Study. Med. Eng. Phys. 2012; 34(6):693–701. [PubMed: 22015316]

13. Lin HT, Kuo LC, Liu HY, Wu WL, Su FC. The Three-Dimensional Analysis of Three Thumb Joints Coordination in Activities of Daily Living. Clin. Biomech. (Bristol, Avon). 2011; 26(4): 371–376.
14. Chang JH, Ho KY, Su FC. Kinetic Analysis of the Thumb in Jar-Opening Activity Among Female Adults. Ergonomics. 2008; 51(6):843–857. [PubMed: 18484399]
15. Sinsel, EW.; Gloekler, DS.; Wimer, BM.; Warren, CM.; Wu, JZ.; Buczek, FL. A Novel Technique Quantifying Phalangeal Interface Pressures at the Hand–Handle Interface. 34th Annual Meeting of the American Society of Biomechanics (ASB-2010); Aug. 18–21; Providence, RI. 2010. Paper #70.
16. Buczek FL, Sinsel EW, Gloekler DS, Wimer BM, Warren CM, Wu JZ. Kinematic Performance of a Six Degree-of-Freedom Hand Model (6DHand) for Use in Occupational Biomechanics. J. Biomech. 2011; 44(9):1805–1809. [PubMed: 21530970]
17. Wu JZ, Sinsel EW, Shroyer JF, Warren CM, Welcome DE, Zhao KD, An KN, Buczek FL. Analysis of the Musculoskeletal Loading of the Thumb During Pipetting—A Pilot Study. J. Biomech. 2014; 47(2):392–399. [PubMed: 24290720]
18. Winter, DA. Biomechanics and Motor Control of Human Movement. 3rd. Hoboken, NJ: Wiley; 2005.
19. Whittle, MW. Gait Analysis: An Introduction. 4th. Edinburgh, UK: Butterworth-Heinemann-Elsevier; 2007.
20. Ateshian G, Ark J, Rosenwasser M, Pawluk R, Soslowsky L, Mow V. Contact Areas in the Thumb Carpometacarpal Joint. J. Orthop. Res. 1995; 13(3):450–458. [PubMed: 7602407]
21. Taylor KF, Lanzi JT, Cage JM, Drake ML. Radial Collateral Ligament Injuries of the Thumb Metacarpophalangeal Joint: Epidemiology in a Military Population. J. Hand Surg. Am. 2013; 38(3):532–536. [PubMed: 23375785]
22. Ritting AW, Baldwin PC, Rodner CM. Ulnar Collateral Ligament Injury of the Thumb Metacarpophalangeal Joint. Clin. J. Sport Med. 2010; 20(2):106–112. [PubMed: 20215892]
23. Samora JB, Harris JD, Griesser MJ, Ruff ME, Awan HM. Outcomes After Injury to the Thumb Ulnar Collateral Ligament—A Systematic Review. Clin. J. Sport Med. 2013; 23(4):247–254. [PubMed: 23615487]
24. Moberg E, Stener B. Injuries to the Ligaments of the Thumb and Fingers; Diagnosis, Treatment and Prognosis. Acta Chir. Scand. 1953; 106(2–3):166–186. [PubMed: 13137829]
25. Bettinger PC, Linscheid RL, Berger RA, Cooney WPR, An KN. An Anatomic Study of the Stabilizing Ligaments of the Trapezium and Trapeziometacarpal Joint. J. Hand Surg. (Am). 1999; 24(4):786–798. [PubMed: 10447171]
26. Neumann DA, Bielefeld T. The Carpometacarpal Joint of the Thumb: Stability, Deformity, and Therapeutic Intervention. J. Orthop. Sports Phys. Ther. 2003; 33(7):386–399. [PubMed: 12918864]
27. Pellegrini VJ. Osteoarthritis of the Thumb Trapeziometacarpal Joint: A Study of the Pathophysiology of Articular Cartilage Degeneration: I. Anatomy and Pathology of the Aging Joint. J. Hand Surg. (Am). 1991; 16(6):967–974. [PubMed: 1748767]

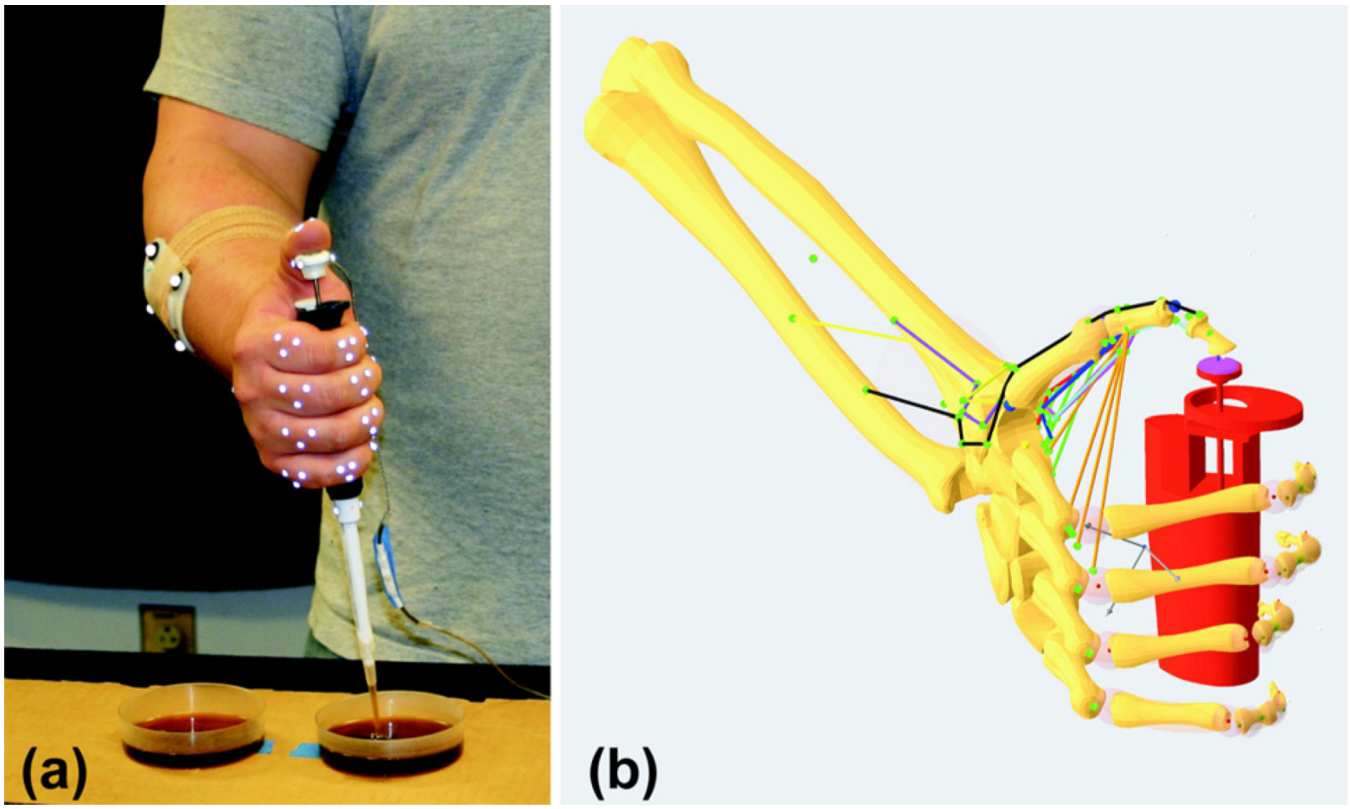

Fig. 1.

Experimental setup and modeling of pipetting. (*a*) A subject operating the pipette during the testing. (*b*) Model of the entire hand with thumb, containing detailed muscle–tendon connections.

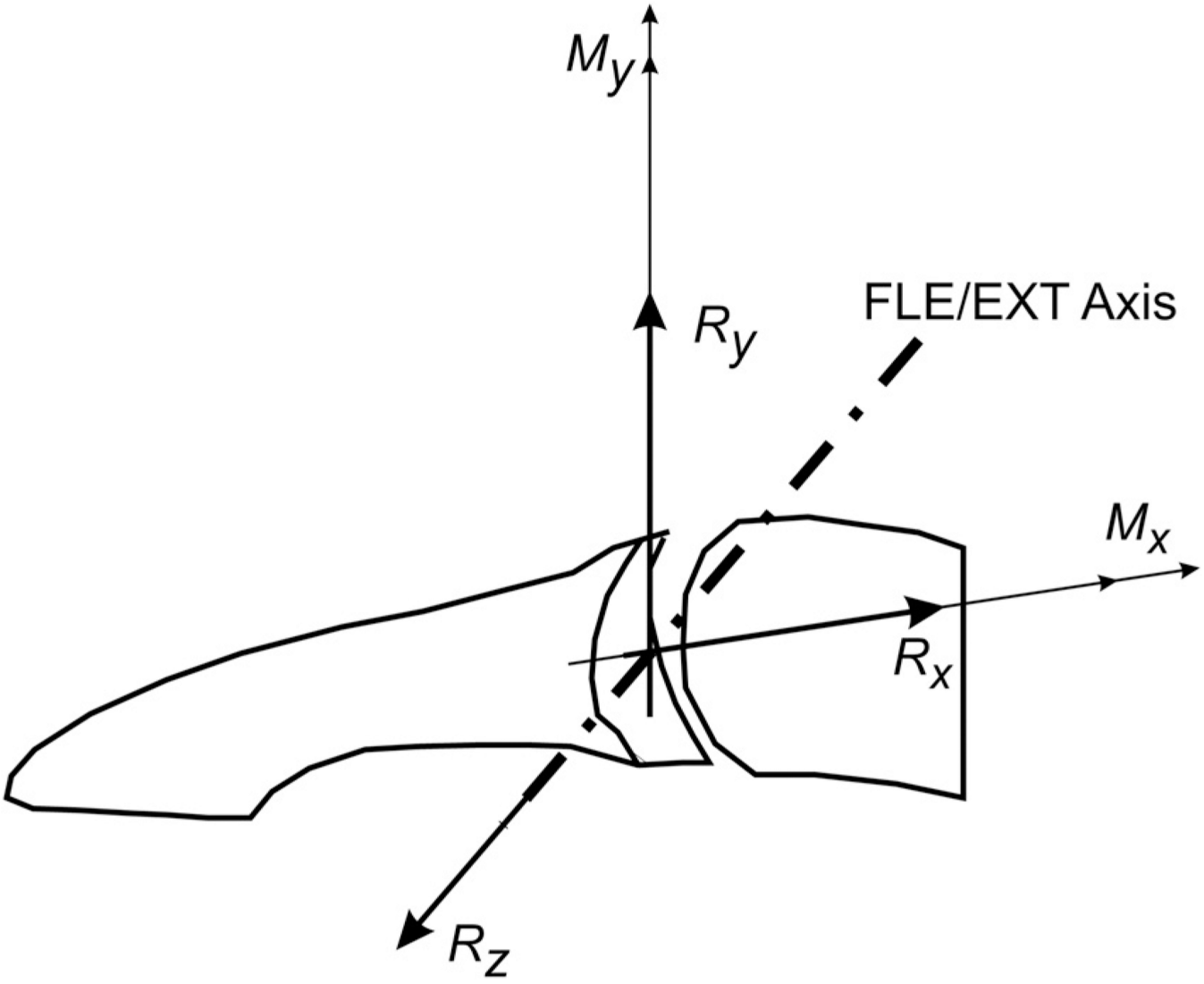

Fig. 2.
Determination of the constraint forces (R_x, R_y, and R_z) and moments (M_x and M_y) in the IP joint

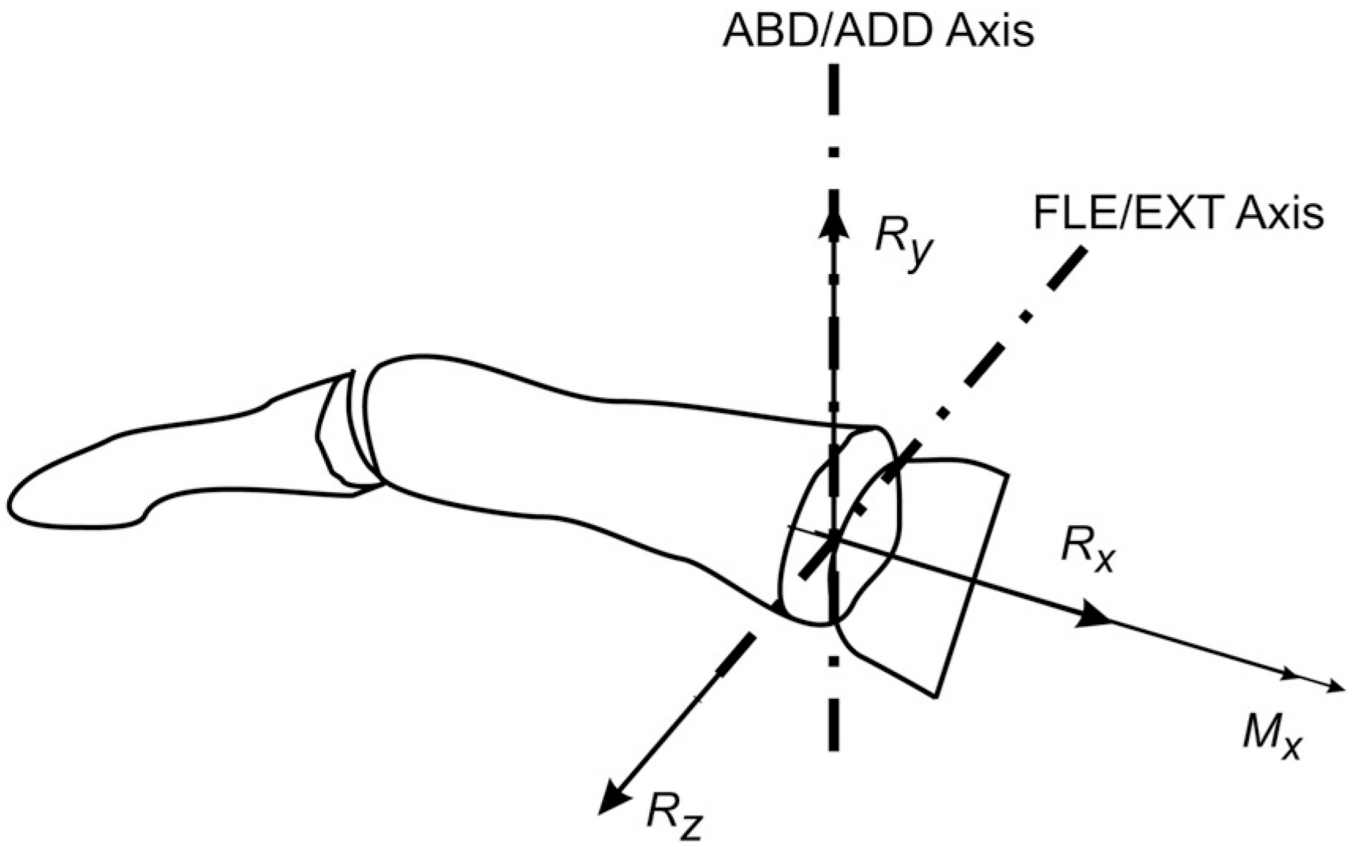

Fig. 3.
Determination of the constraint forces (R_x, R_y, and R_z) and moment (M_x) in the MP joint

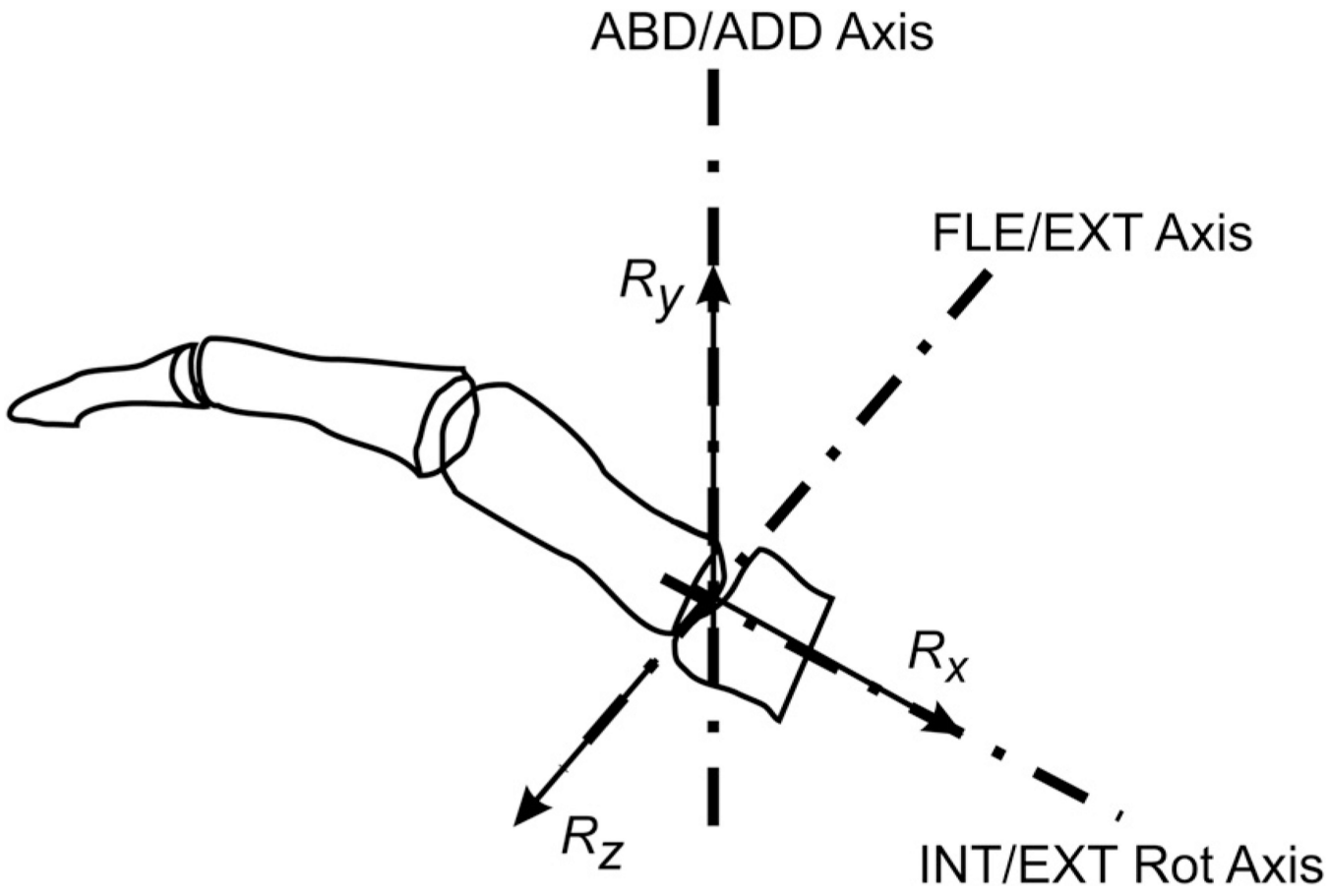

Fig. 4.
Determination of the constraint forces (R_x, R_y, and R_z) in the CMC joint

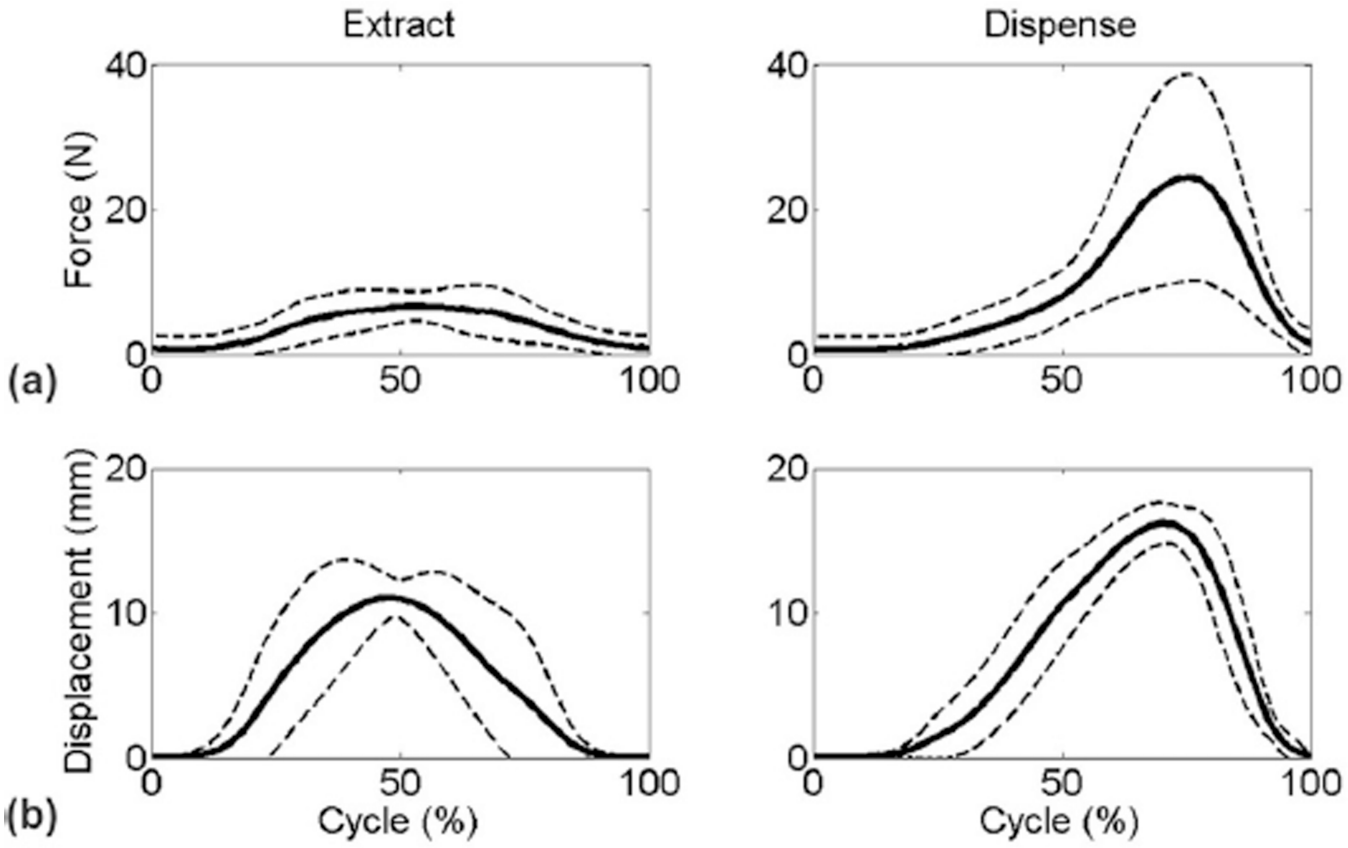

Fig. 5.

Histories of the push force and button displacement during the extraction and dispensing cycles. (*a*) The push force as a function of pipetting cycle. (*b*) The button displacement as a function of pipetting cycle. The solid lines represent the mean values of all eight subjects' data and the dotted lines are the standard deviations.

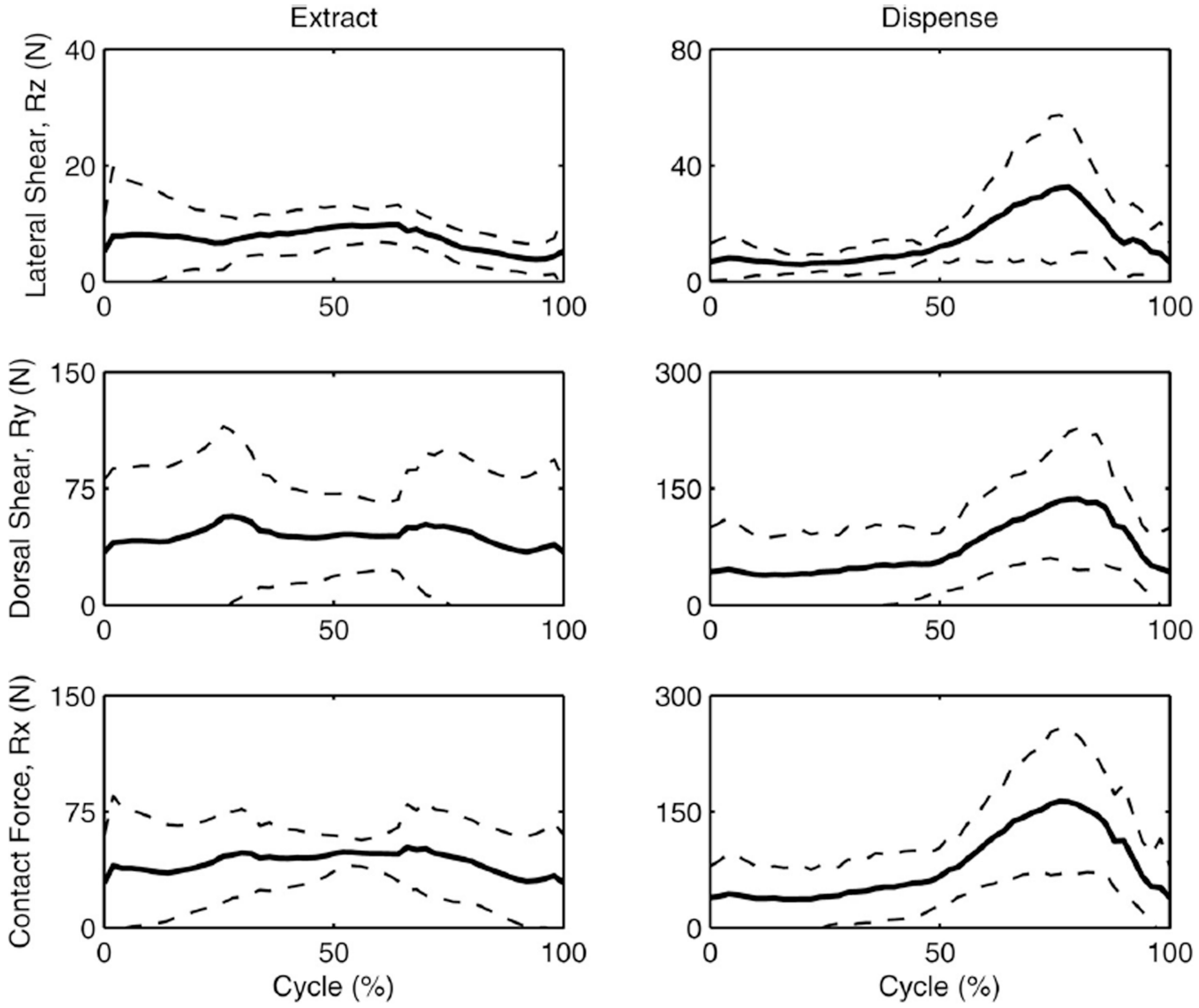

Fig. 6.

Variations in the CMC joint constraint forces during the extraction and dispensing cycles. The left and right columns of the plots show the forces in the extraction and dispensing phases, respectively. The mean values are shown in solid lines, whereas the standard deviations of the data are shown in dotted lines.

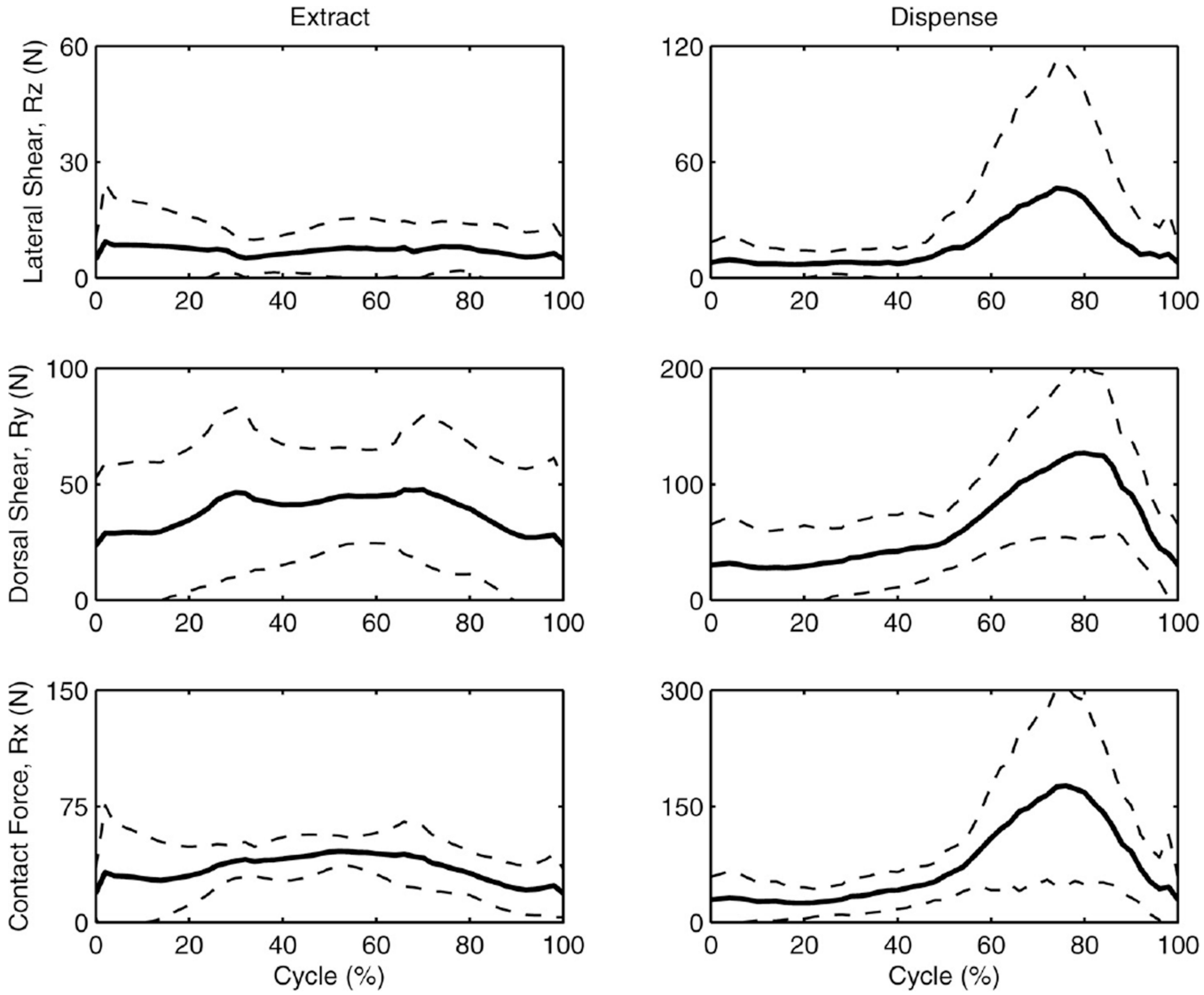

Fig. 7.

Variations in the MP joint constraint forces during the extraction and dispensing cycles. The left and right columns of the plots show the forces in the extraction and dispensing phases, respectively. The mean values are shown in solid lines, whereas the standard deviations of the data are shown in dotted lines.

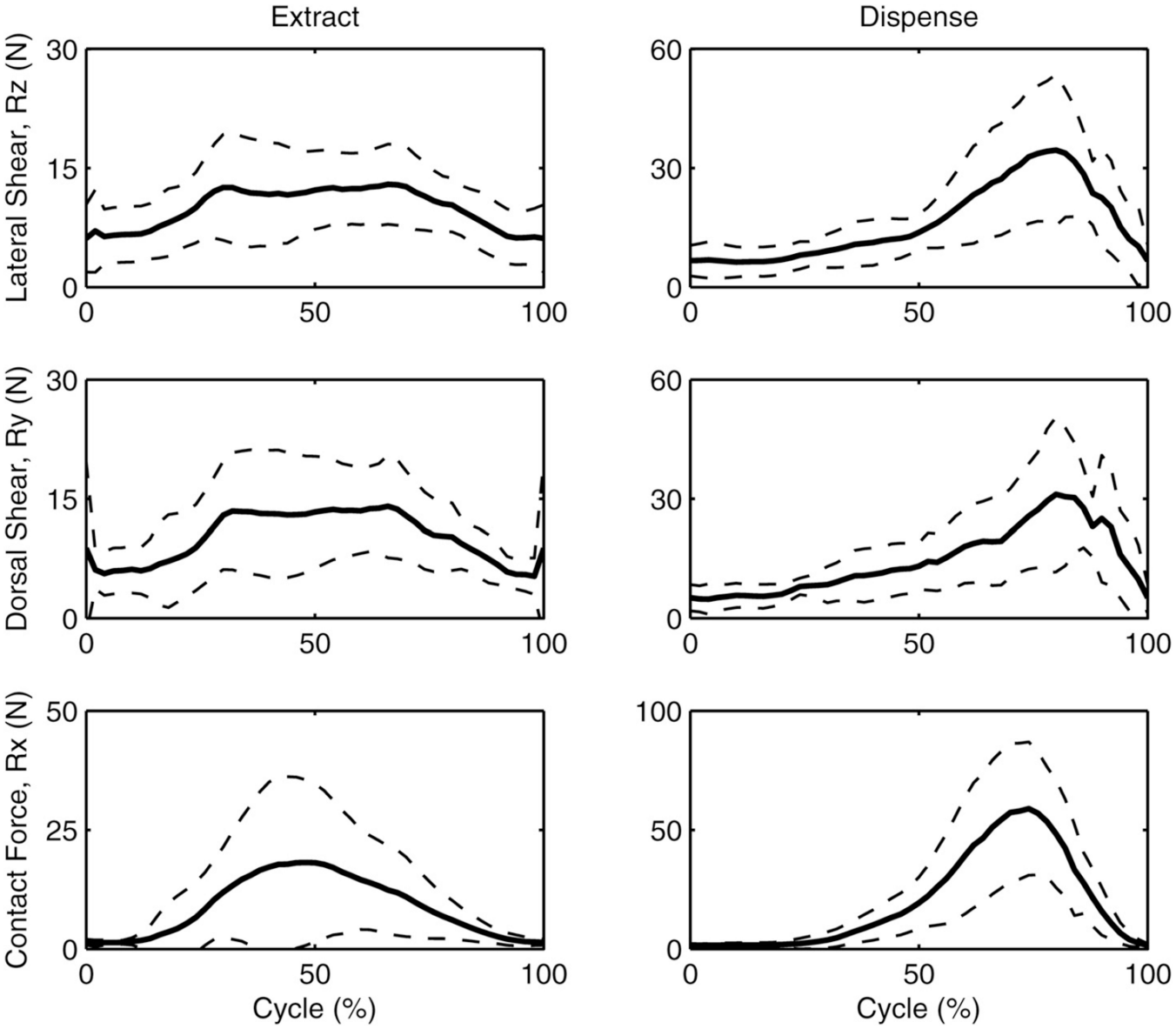

Fig. 8.

Variations in the IP joint constraint forces during the extraction and dispensing cycles. The left and right columns of the plots show the forces in the extraction and dispensing phases, respectively. The mean values are shown in solid lines, whereas the standard deviations of the data are shown in dotted lines.

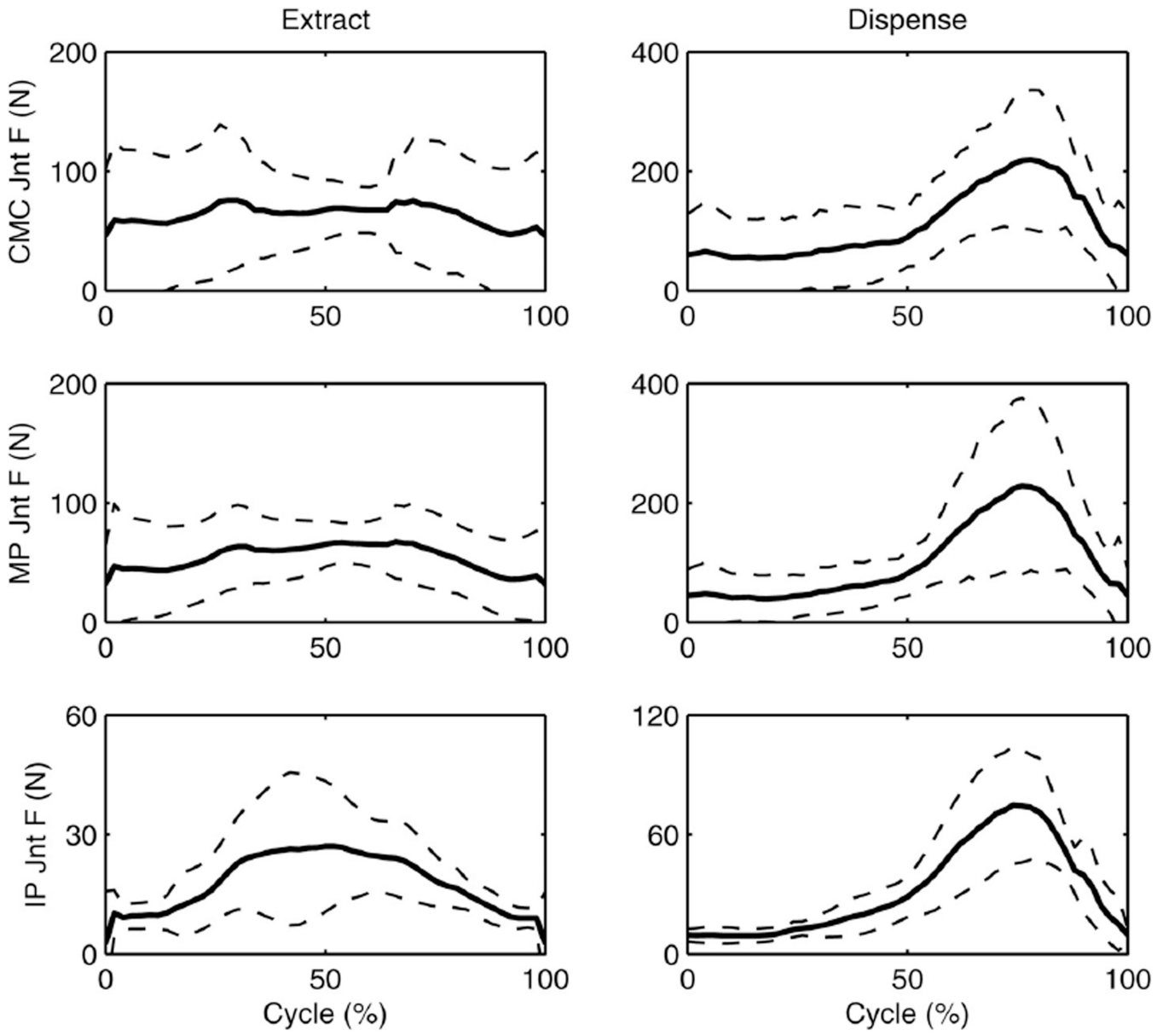

Fig. 9.

Variations in the resultant constraint forces in the CMC, MP, and IP joints during the extraction and dispensing cycles

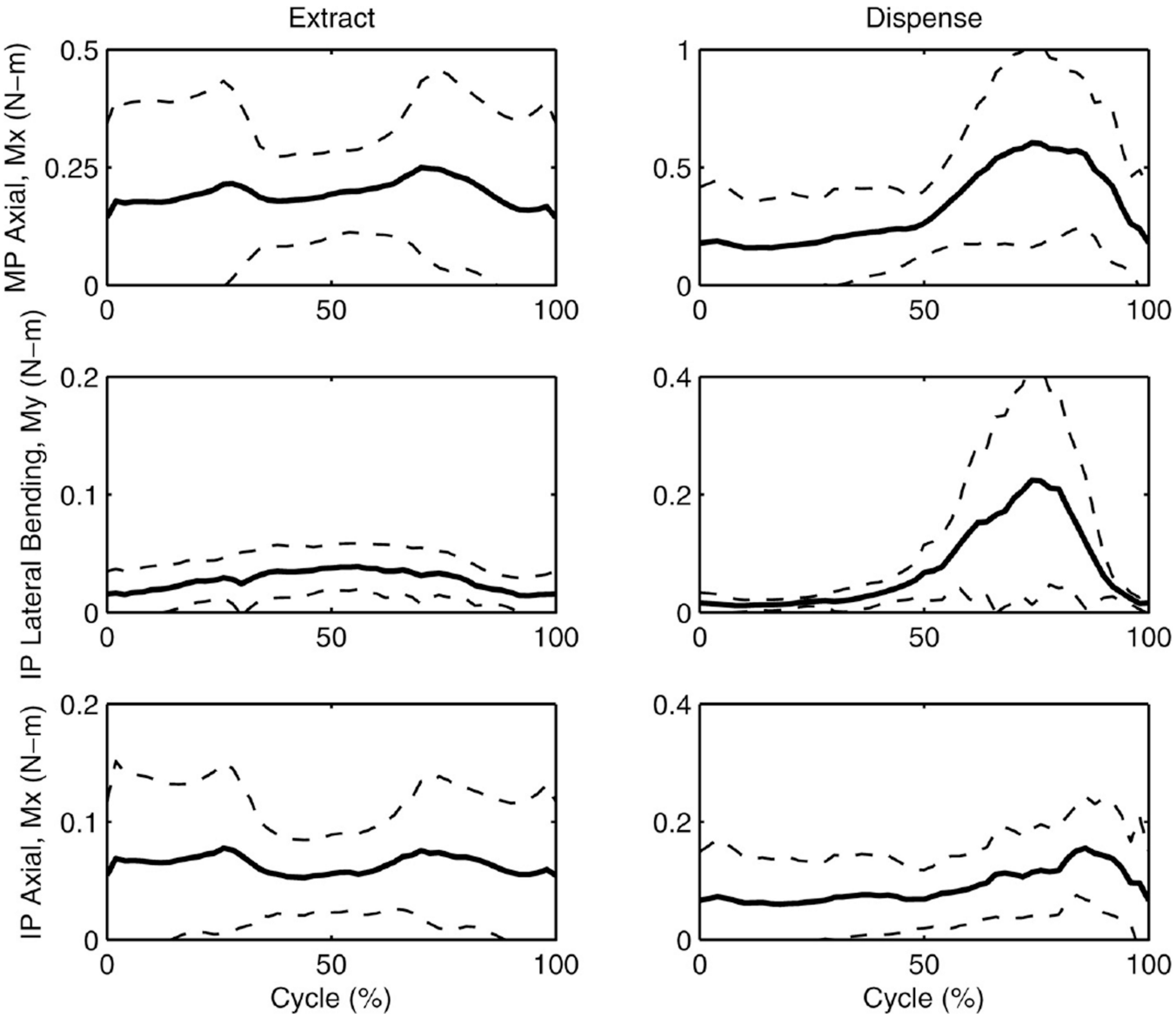

Fig. 10.

Variations in the constraint moments in the IP and MP joints during the extraction and dispensing cycles

Table 1

Comparison of the constraint forces and moments in the IP, MP, and CMC joints obtained in the current study with those by Cooney and Chao [9]

		IP	MP	CMC
Tip pinch (9.8 N) Cooney and Chao [9]	Compression (R_x) (N)	29.6	54.2	97.3
	Lateral shear (R_y) (N)	2.3	19.4	17.2
	Dorsal shear (R_z) (N)	1.2	6.5	11.5
	Axial rot. M (M_x) (N m)	0.0	0.0	0.2
	Lateral bending M (M_y) (N m)	0.0	0.0	0.0
Key pinch (9.8 N) Cooney and Chao [9]	Compression (R_x) (N)	28.7	55.3	111.4
	Lateral shear (R_y) (N)	1.0	4.4	2.0
	Dorsal shear (R_z) (N)	7.0	19.4	18.6
	Axial rot. M (M_x) (N m)	0.0	0.1	0.2
	Lateral bending M (M_y) (N m)	0.0	0.0	0.0
Grasp (98 N) Cooney and Chao [9]	Compression (R_x) (N)	183.8	582.6	1223.0
	Lateral shear (R_y) (N)	0.0	39.2	69.1
	Dorsal shear (R_z) (N)	38.7	199.9	113.7
	Axial rot. M (M_x) (N m)	0.0	1.1	1.4
	Lateral bending M (M_y) (N m)	0.0	0.0	0.0
Pipetting (25 N) Current study	Compression (R_x) (N)	59.0	178.0	160.0
	Lateral shear (R_y) (N)	30.0	128.0	133.0
	Dorsal shear (R_z) (M)	34.0	47.0	33.0
	Joint force mag. (F) (N)	74.4	224.2	210.7
	Axial rot. M (M_x) (N m)	0.2	0.6	0.0
	Lateral bending M (M_y) (N m)	0.2	0.0	0.0